

Gas-phase reaction of OH radicals with phenol

Torsten Berndt and Olaf Böge

Institut für Troposphärenforschung e.V., Permoserstraße 15, 04318, Leipzig, Germany

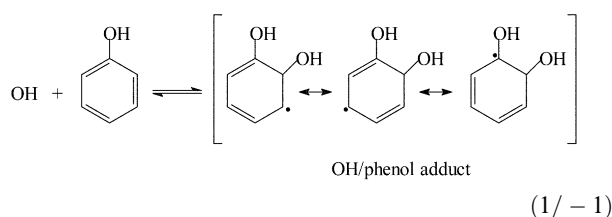
Received 21st August 2002, Accepted 15th November 2002

First published as an Advance Article on the web 4th December 2002

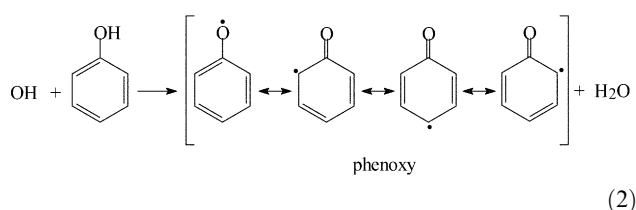
The gas-phase reaction of OH radicals with phenol was investigated in a flow tube in the temperature range of 266–364 K and a pressure of 100 mbar. The product formation was followed by on-line FT-IR spectroscopy and GC-MS measurements. Newly formed particles were detected by means of a low-pressure CPC (condensation particle counter). In the presence of O₂, OH radicals were generated *via* the reaction sequence H + O₂ + M → HO₂ + M, HO₂ + NO → OH + NO₂ and in the absence of O₂ *via* H + NO₂ → OH + NO. For evaluation of a possible competing process, the rate constant for H + phenol was measured, $k(\text{H} + \text{phenol}) = (2.5 \pm 1.5) \times 10^{-13} \text{ cm}^3 \text{ molecule}^{-1} \text{ s}^{-1}$ (295 ± 2 K, 25 mbar He). Under the experimental conditions used the H-atom reaction does not compete with the reaction of OH radicals with phenol. At 295 K, the product distribution was studied for different O₂, NO and NO₂ concentrations. Identified products were catechol, *o*-nitrophenol and *p*-benzoquinone. Under all experimental conditions catechol represented the main product. The measured dependence of the catechol yield on NO and NO₂ for constant O₂ concentrations allowed an estimate of the reactivity of the OH/phenol adduct towards O₂, NO and NO₂, $k(\text{adduct} + \text{O}_2)/k(\text{adduct} + \text{NO}) > 10^{-3}$ and $k(\text{adduct} + \text{O}_2)/k(\text{adduct} + \text{NO}_2) = (1.4 \pm 0.5) \times 10^{-4}$. For constant gas composition, in the absence of additional NO₂, the product distribution was measured for different temperatures. With increasing temperature the catechol yield increased from 0.37 ± 0.06 (266 K) to 0.87 ± 0.04 (364 K). The yields of *o*-nitrophenol and *p*-benzoquinone were nearly constant. Below 295 K, with decreasing temperature enhanced formation of newly formed particles was observed. For realistic atmospheric conditions, a catechol yield of 0.73–0.78 (295 K) can be recommended from this study.

Introduction

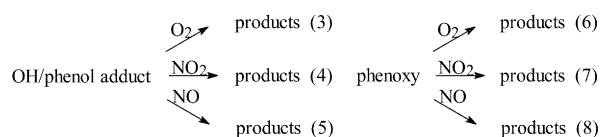
Atmospheric degradation of benzene and its alkylated derivatives (toluene, xylenes, *etc.*) in the gas phase is exclusively initiated by the reaction with OH radicals.¹ Ring-retaining products of this reaction are phenol-type compounds (phenol, cresols, dimethylphenols, *etc.*).² For benzene, experimentally obtained phenol yields under nearly atmospheric conditions are in the range 0.24–0.53.^{3–6} The fate of the formed phenol-type compounds is governed by the reaction with OH and NO₃ radicals.⁷ For phenol, the reaction with OH radicals proceeds *via* a reversible addition step forming the OH/phenol adduct (for simplification only the attack in *ortho* position is shown).



and *via* H-atom abstraction predominantly from the OH substituent group forming phenoxy radicals.^{2,8}

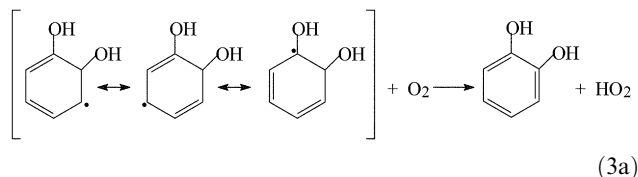


Kinetic data for pathways (1), (–1) and (2) exist in the literature.^{9,10} At 298 K the addition pathway (1) dominates over the abstraction pathway (2) and the ratio $k_1/(k_1 + k_2)$ is in the range 0.76–0.87.^{9,10} Kinetic investigations concerning the subsequent reaction of the OH/phenol adduct with O₂, NO₂ and NO (rate constants in units of cm³ molecule^{–1} s^{–1}: $k_3 = (3.0 \pm 0.7) \times 10^{-14}$ (323 K), $k_4 = (3.4 \pm 0.6) \times 10^{-11}$ (331 K) and $k_5 < 7 \times 10^{-14}$ (316–332 K), respectively)^{9,10} clearly favour the reaction with O₂ under atmospheric conditions. Analogous studies for the reaction of phenoxy radicals with O₂, NO₂ and NO ($k_6 < 2 \times 10^{-18}$ (280–500 K)¹¹ or $k_6 < 5 \times 10^{-21}$ (296 K),¹² $k_7 = (2.08 \pm 0.15) \times 10^{-12}$ (296 K)¹² and $k_8 = (1.88 \pm 0.16) \times 10^{-12}$ (296 K),¹² respectively) indicate that the fate of phenoxy radicals in the atmosphere is not governed by the reaction with O₂, but by the reaction with NO_x or possibly other species such as O₃.

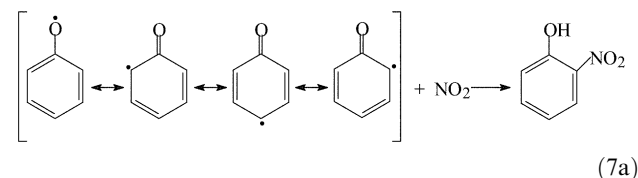


To the authors' knowledge, two product studies are reported so far concerning the gas-phase reaction of OH radicals with phenol.^{7,13} These experiments were performed in batch reactors (room temperature, 1 bar synthetic air) using photolysis of methyl nitrite for OH generation. The yields of the identified products were: catechol (0.804 ± 0.121),¹³ *o*-nitrophenol (0.067 ± 0.015)⁷ and (0.058 ± 0.010)¹³ as well as *p*-benzoquinone (0.037 ± 0.012).¹³ An aqueous-phase study of the reaction of OH radicals with phenol in the presence of NO₂ at pH = 3 yielded *o*- and *p*-nitrophenol with formation yields of 0.18 ± 0.08 and 0.12 ± 0.08, respectively, as well as traces

of catechol.¹⁴ Generally, catechol formation can be described starting from the OH/phenol adduct (*ortho*-position) assuming H-abstraction by O₂.¹³



The formation of *o*-nitrophenol is attributed to the reaction of phenoxy radicals with NO₂.⁷

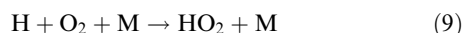


Note that the given pathway represents an overall reaction only. At least an intramolecular H-atom transfer step is needed to produce a phenol-type substance starting from phenoxy radicals.

The aim of the present study was to determine the products of the reaction of OH radicals with phenol in dependence on gas composition (O₂, NO and NO₂ concentration) and temperature. The experimental finding that k_1 , k_{-1} , k_2 and k_3 are pressure independent above 30–50 mbar (Ar as dilution gas)¹⁰ justifies the use of a total pressure of 100 mbar and allows the application of the results to atmospheric pressure. The measurement of newly formed particles should clarify the possible formation of condensable substances not detectable in the gas phase. From the sum of all experimental findings under different conditions more insight into the mechanism of the reaction of OH radicals with phenol is expected. Additionally, for the evaluation of a possible competing process under the applied reaction conditions, the rate constant for the reaction of H-atoms with phenol was measured.

Experimental

The experiments were carried out at a pressure of 100 mbar in a quartz glass flow tube (4.0 cm id, total length: 100 cm) surrounded with a thermo-jacket allowing operation in the temperature range of 266–364 K. In the presence of sufficient O₂ in the reaction gas ([O₂] = 1.68×10^{18} molecule cm⁻³) OH radicals were produced *via* the reaction sequence:



In these experiments NO additions were in the range $(9.8\text{--}244) \times 10^{12}$ molecule cm⁻³. In the absence of O₂ ([O₂] < 2×10^{13} molecule cm⁻³, [NO₂] = $(1.8\text{--}17.2) \times 10^{13}$ molecule cm⁻³) OH radicals were produced *via*:



Approximately 50 cm downstream of the point for the entrance of phenol and the additions diluted in the carrier gas, in a side-arm H-atoms were generated in a commercial microwave discharge (SAIREM GMP 03 K/SM) using a mixture of 0.012–0.023 vol% H₂ in He.

The main part of the reaction gas was pumped continuously through a White cell (volume: 2050 cm³, optical path length: 10 m) for FT-IR analysis (Nicolet Magna 750) using an instrumental resolution of 8 cm⁻¹ averaging 200–2000 scans. At 100 mbar and 295 K, calibrated reference spectra of the reaction products (catechol, *o*-nitrophenol and *p*-ben-

zoquinone) were obtained by flushing out the gas phase over the solid sample by the carrier gas over a time period of 1.5–23 h. During this period, FT-IR spectra of the resulting gas mixture were measured in different intervals and in the end of that the mass differences of the solid sample was determined. Under conditions of nearly constant sublimation in the whole time period ($\Delta m/m$ is small, surface of the solid stays nearly unchanged, constant temperature), from the mass difference and the total volume of the gas stream an averaged concentration of the sublimated substance can be calculated setting the FT-IR spectra on an absolute scale. Using this approach, the reproducibility of the results was found to be reasonable and determined absorption cross sections for the strongest absorption bands were (base 10, unit: 10⁻¹⁹ cm² molecule⁻¹); catechol: 4.0 ± 0.3 at 1273 cm⁻¹, *o*-nitrophenol: 3.9 ± 0.4 at 1342 cm⁻¹ and *p*-benzoquinone: 9.1 ± 3.2 at 1680 cm⁻¹. Error limits represent two standard deviations. Because of too low sublimation vapour pressure, for *p*-nitrophenol this procedure did not work. Appropriate cross sections given in the literature¹³ were measured with an instrumental resolution of 1 cm⁻¹ making a reasonable comparison with the data of this study (instrumental resolution: 8 cm⁻¹) impossible.

For on-line GC-MS analysis (HP 5890 with HP MSD 5971), a smaller part of the gas stream was pumped continuously through a GC loop connected with the flow tube by means of a heated transfer line. For product separation, a 30 m, 0.25 mm id column (HP 5MS) was chosen. Using the corresponding ion traces, *o*-nitrophenol ($m/z = 139$ u) and *p*-benzoquinone ($m/z = 108$ u) were detected efficiently allowing the analysis of both substances down to flow-tube concentrations of approximately 10¹⁰ molecule cm⁻³. For signal calibration, GC-MS chromatograms and FT-IR spectra from the same sample were measured simultaneously using the determined concentration from the FT-IR measurement as the reference value (see the paragraph above). Because of probably effective wall loss in the sampling device, the determination of catechol was not successful using this GC method. Also for the GC-MS analysis of *o*-nitrophenol and *p*-benzoquinone, wall processes affecting the determined concentrations under reaction conditions (presence of NO_x) can not fully be ruled out.

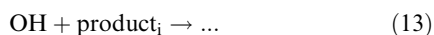
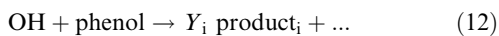
Furthermore, few runs were performed with particle measurements or with cryo-trapping of the reaction products. For particle measurements, a modified CPC (condensation particle counter, TSI 7610) was used operating with FC 43 (perfluorotributylamine) as working fluid.¹⁵ The CPC was directly attached to the flow tube approximately 45 cm downstream the mixing point of the reactants resulting in a residence time of 0.63 s before particle counting. Before measurements, the counting efficiency of the CPC at 100 mbar was determined using an aerosol electrometer in a low-pressure calibration set-up.^{16,17} For cryo-trapping, for a time period of 1 h the whole gas stream was pumped through a gas trap held at liquid argon temperature. After disconnecting the trap from the flow tube, the frozen material was immediately dissolved in methanol and analysed by GC-MS (HP 6890 with HP MSD 5973). For product separation, an identical column as used for the on-line GC-MS analysis was chosen.

For the metering of phenol into the flow tube the same approach was used as described for the signal calibration of the reaction products. The resulting phenol concentration in the tube was permanently controlled by FT-IR measurements. The phenol source was found to be stable over a time period of days.

The gas flows were set by calibrated mass flow controllers (MKS 1259) and the pressure in the tube and in the gas cell was measured using capacitive manometers (Baratron). The total gas flow was set at 5000 standard cm³ min⁻¹ resulting in a bulk residence time in the reaction zone of the flow tube

of 0.7 s (295 K). The temperature of the gas stream was measured by means of a thermocouple located in the middle of the flow tube approximately 3 cm downstream the point for the entrance of the H-atoms.

The initial concentration of phenol was $(5.9\text{--}6.7) \times 10^{13}$ molecule cm^{-3} and the amount of reacted phenol was in the range $(4.8\text{--}8.9) \times 10^{12}$ molecule cm^{-3} . Consecutive reactions of products with OH radicals were taken into consideration in the following way. Assuming the simplified reaction scheme,

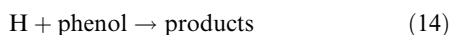


by dividing of the rate laws for the product_i and phenol, eqn. (I) follows.

$$\frac{d[\text{product}_i]}{d[\text{phenol}]} = -Y_i + \frac{k_{13}[\text{product}_i]}{k_{12}[\text{phenol}]} \quad (\text{I})$$

Eqn. (I) was solved numerically by an explicit extrapolation method¹⁸ connected with a Newton-technique¹⁸ for the determination of the formation yield Y_i . Neglecting $\frac{k_{13}[\text{product}_i]}{k_{12}[\text{phenol}]}$, eqn. (I) represents the definition of the formation yield for product_i in the absence of consecutive processes and by integration follows $Y_i = [\text{product}_i]/\Delta[\text{phenol}]$. Here $\Delta[\text{phenol}]$ stands for the reacted phenol. For an evaluation of the importance of the correction, $\frac{k_{13}[\text{product}_i]}{k_{12}[\text{phenol}]}$, the needed rate constants were taken from literature (in units of $\text{cm}^3 \text{ molecule}^{-1} \text{ s}^{-1}$): $k_{12} = (2.8 \pm 0.6) \times 10^{-11}$ (296 K),¹⁹ $k_{13,\text{catechol}} = (1.04 \pm 0.21) \times 10^{-10}$ (300 K),²⁰ $k_{13,o\text{-nitrophenol}} = 9 \times 10^{-13}$ (room temperature),⁸ $k_{13,p\text{-benzoquinone}} = (4.6 \pm 0.9) \times 10^{-11}$ (300 K).²⁰ Because of the low reactivity of *o*-nitrophenol, the correction for the consecutive reaction *via* pathway (13) was not necessary. For *p*-benzoquinone, approximately 5–10% of this substance reacted with OH radicals *via* pathway (13). Because of a total uncertainty of 50% in the determination of *p*-benzoquinone, this effect was neglected. Therefore, the product yields of *o*-nitrophenol and *p*-benzoquinone were determined according to $Y_i = [\text{product}_i]/\Delta[\text{phenol}]$. For catechol, up to 25% of this substance reacted with OH radicals *via* pathway (13) making the determination of the product yield with the help of eqn. (I) necessary. For the temperature-dependent measurements, Arrhenius expressions for k_{12} and $k_{13,\text{catechol}}$ were needed. Because only for k_{12} this information is available in the literature,²¹ $k_{13,\text{catechol}}/k_{12}$ was assumed to be temperature-independent.

Additionally, the rate constant for the reaction of H-atoms with phenol was measured. The experimental approach used has been described elsewhere,²² here only a brief discussion is given. The experiments were performed in a quartz glass flow tube (2.0 cm id, length: 50 cm) at 295 ± 2 K and a total pressure of 25 mbar He. H atoms were generated by means of a microwave discharge (SAIREM GMP 03 K/SM). For the determination of the rate constant the relative rate technique was employed and mesitylene served as the reference substance.



From the measured signals without conversion, index “0”, and in the presence of H-atoms, index “t”, eqn. (II) follows:

$$\frac{k_{14}}{k_{15}} = \frac{\ln([\text{phenol}]_0/[\text{phenol}]_t)}{\ln([\text{mesitylene}]_0/[\text{mesitylene}]_t)} \quad (\text{II})$$

From the ratio k_{14}/k_{15} , the desired rate constant k_{14} followed using the literature value for k_{15} .²² The disappearance of both substances was observed using a quadrupole mass spectrometer (Balzers QMA 200) operating in the 70 eV EI mode. Changing consumption of the organic substances was achieved

by changing the H-atom concentration using variable H_2 contents in the gas stream for the microwave discharge.

The gases used had stated purities as follows: He (99.999%), O_2 (99.9996%), Ar (99.999%) (Linde), H_2 (99.999%), NO (0.5 vol% mixture in N_2) (Messer Griesheim) and NO_2 (99.5%) (Merck). Phenol (>99.99%), catechol (>99%), mesitylene (99.8%), *o*-nitrophenol (>99%), *p*-nitrophenol (>99%), 4-nitrocatechol (>98%) and *p*-benzoquinone (>99.5%) (Fluka) were used as purchased. 3-Nitrocatechol was synthesized by treatment of catechol with acetic anhydride forming the catechol monoacetate, followed by nitration in glacial acetic acid, separation of the desired isomer and saponification as described by Berti.²³

Results and discussion

Kinetics of the reaction H + phenol

Because OH radicals were generated from H-atoms *via* the sequence of pathways (9) and (10) or *via* pathway (11), a possible contribution of the reaction of H-atom with phenol for the total conversion of phenol had to be clarified. In the literature, rate constants for H + phenol are only available for high temperature conditions.²⁴ Here, the rate constant was obtained at 295 ± 2 K and a total pressure of 25 mbar He using the relative rate technique. Initial concentrations of 2.8×10^{13} molecule cm^{-3} for phenol and 1.1×10^{13} molecule cm^{-3} for mesitylene were applied. For the MS detection of phenol the ion trace at $m/z = 94$ u and for mesitylene at $m/z = 105$ u was measured. First, the reaction products of the reaction of H-atoms with the organic substances were analysed to be sure that the chosen ion traces were not afflicted by the products. Identified products were 2-cyclohexenol, cyclohexanol, 2-cyclohexenone and cyclohexanone arising from phenol as well as the 1,3,5-trimethyl derivatives of cyclohexadiene, cyclohexene and cyclohexane arising from mesitylene.²² In the 70 eV EI spectra of all these products there are no appreciable signals at $m/z = 94$ u and $m/z = 105$ u. In Fig. 1 the experimental findings are plotted according to eqn. (II). The slope k_{14}/k_{15} was

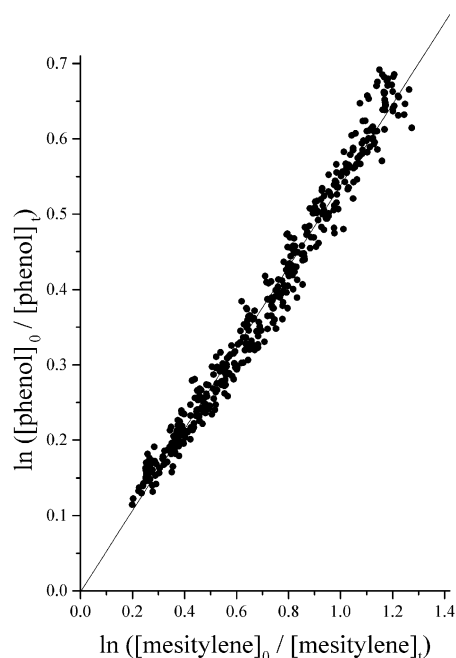


Fig. 1 Experimental data for the determination of the relative rate constant of the reaction of H-atoms with phenol using mesitylene as the reference substance; $T = 295 \pm 2$ K, $p = 25$ mbar He. Data are plotted according to eqn. (II).

found to be 0.540 ± 0.008 , the intercept was -0.0015 ± 0.006 , and the correlation coefficient was 0.989. Uncertainties represent 2σ . Using a value $k_{15} = (4.6 \pm 2.7) \times 10^{-13} \text{ cm}^3 \text{ molecule}^{-1} \text{ s}^{-1}$ from literature,²² $k_{14} = (2.5 \pm 1.5) \times 10^{-13} \text{ cm}^3 \text{ molecule}^{-1} \text{ s}^{-1}$ follows.

As a result of kinetic investigations of the reaction of H-atoms with benzene at 298 K no pressure dependence in the range 16–133 mbar Ar was observed.²⁵ It was concluded that the rate constant was in the high pressure limit even at 16 mbar. By analogy for H + phenol, it can be assumed that k_{14} represents a high pressure value also. Therefore, the measured rate constant k_{14} is applicable for the conditions at 100 mbar of this study.

Mechanistic informations

From the detected products it can be speculated that the reaction of H-atoms with phenol proceeds, on the one hand, *via* ring addition producing 2-cyclohexenol and cyclohexanol after consecutive H-atom additions. This would be a similar behaviour as described for methyl substituted benzenes.²² On the other hand, also H-abstraction can be postulated producing primary phenoxy radicals and H_2 . The detected 2-cyclohexenone and cyclohexanone can be regarded as stable products of phenoxy radicals from further reactions with H-atoms. Despite the speculative nature and the uncertainty of the primary steps, the attack of H-atoms can be described tentatively in the same manner as the attack of OH radicals, namely by ring addition and by H-abstraction from the OH substituent group, *cf.* the introductory paragraph.

Cryo-trapping

The intention of experiments with cryo-trapping was to get a qualitative overview of the products. Experimental conditions were similar to those with FT-IR and on-line GC-MS analysis, see later. Fig. 2 shows a typical GC-MS chromatogram from a cryo-trapping experiment ($T = 295 \text{ K}$, $[\text{O}_2] = 1.68 \times 10^{18} \text{ molecule cm}^{-3}$, $[\text{NO}] = 4.1 \times 10^{13} \text{ molecule cm}^{-3}$, $[\text{phenol}] = 6.5 \times 10^{13} \text{ molecule cm}^{-3}$, $\Delta[\text{phenol}] \sim 5 \times 10^{12} \text{ molecule cm}^{-3}$). Detected products were *p*-benzoquinone, *o*-nitrophenol,

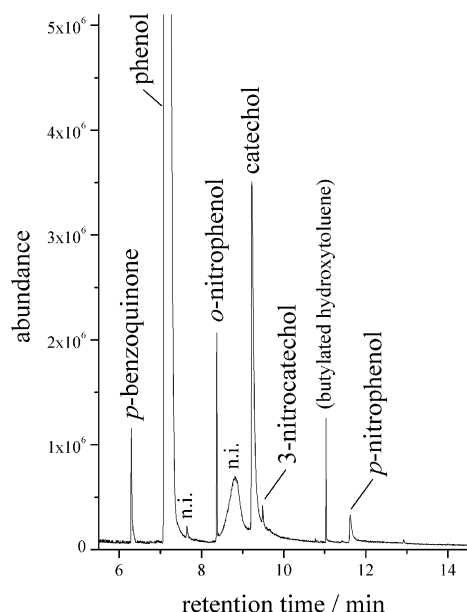


Fig. 2 GC-MS analysis of a cryo-trapping experiment from the reaction of OH radicals with phenol in the presence of O_2 . Products were assigned using the mass spectra of the reference substances. “n.i.” stands for “not identified”.

catechol, 3-nitrocatechol and *p*-nitrophenol. The identified butylated hydroxytoluene came from the solvents itself. The unambiguous assignment of the several products was achieved using the mass spectra of the reference substances. For experiments performed in the absence of O_2 ($T = 295 \text{ K}$, $[\text{NO}_2] = 4.1 \times 10^{13} \text{ molecule cm}^{-3}$, $[\text{phenol}] = 6.5 \times 10^{13} \text{ molecule cm}^{-3}$, $\Delta[\text{phenol}] \sim 8 \times 10^{12} \text{ molecule cm}^{-3}$), the same product pattern was visible as found for conditions in the presence of O_2 . The signal intensity for catechol, however, was lowered compared to that for the nitrophenols. Repeated injections of the same sample of dissolved reaction products showed a clear decrease of the catechol signal and an increase especially of the *p*-nitrophenol signal with time. Obviously, in the condensed phase further reactions took place probably initiated by NO_2 . This fact and the unknown collecting efficiency for the different products in the cryo-trap prevented a determination of product yields.

Gas-phase products in the presence of O_2

In these experiments the O_2 concentration was $1.68 \times 10^{18} \text{ molecule cm}^{-3}$ and the initial phenol concentration $6.5 \times 10^{13} \text{ molecule cm}^{-3}$. A comparison of the H-atoms lifetimes with respect to the reaction with O_2 *via* pathway (9) and phenol *via* pathway (14) of $4 \times 10^{-6} \text{ s}$ and 0.06 s, respectively, shows that the reaction of H-atoms with phenol was negligible under these conditions. The rate constant needed for pathway (9) was taken from the literature, $k_9(\text{M}) = 6.1 \times 10^{-32} \text{ cm}^6 \text{ molecule}^{-2} \text{ s}^{-1}$ at 298 K ($\text{M} = \text{N}_2$ here applied for the O_2/He mixture),²⁶ and that for pathway (14) from the present study. The amount of reacted phenol was in the range $(4.9\text{--}7.9) \times 10^{12} \text{ molecule cm}^{-3}$.

Fig. 3 demonstrates the determination of product yields by means of FT-IR measurements ($T = 295 \text{ K}$, $[\text{O}_2] = 1.68 \times 10^{18} \text{ molecule cm}^{-3}$, $[\text{NO}] = 4.9 \times 10^{13} \text{ molecule cm}^{-3}$, $\Delta[\text{phenol}] = 6.2 \times 10^{12} \text{ molecule cm}^{-3}$). In the original difference spectrum (upper part) absorptions from consumed substances (phenol, NO) appear as negative bands and product absorptions as positive bands. After addition of phenol bands and subtraction of catechol bands, only the bands arising from

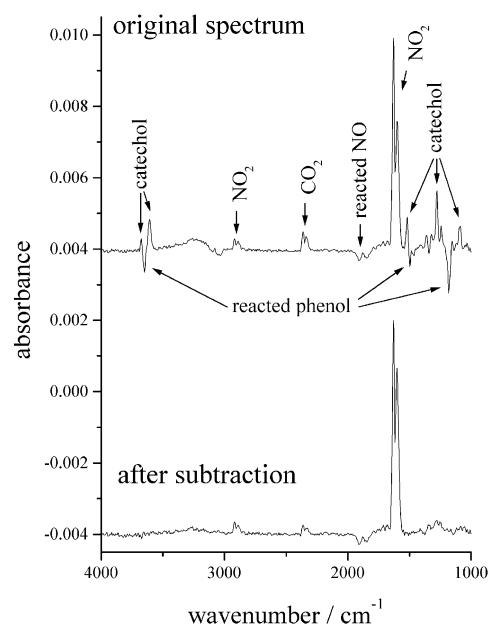


Fig. 3 Upper part: Typical FT-IR spectrum from the reaction of OH radicals with phenol in the presence of O_2 ; $T = 295 \text{ K}$, $[\text{NO}] = 4.9 \times 10^{13} \text{ molecule cm}^{-3}$, $\Delta[\text{phenol}] = 6.2 \times 10^{12} \text{ molecule cm}^{-3}$. Lower part: Residual spectrum after addition of phenol bands and subtraction of catechol bands using reference spectra each.

background CO_2 , NO_2 and from reacted NO remained (lower part). There were no clear indications for further products, such as *p*-benzoquinone and *o*-nitrophenol. The weak absorptions in the range $1500\text{--}1000\text{ cm}^{-1}$ were unspecific and probably influenced by the procedure of spectral subtraction. Indeed, *p*-benzoquinone and *o*-nitrophenol were unambiguously identified by on-line GC-MS analysis. The FT-IR detection limits were estimated to be $3 \times 10^{11}\text{ molecule cm}^{-3}$ for *p*-benzoquinone and $7 \times 10^{11}\text{ molecule cm}^{-3}$ for *o*-nitrophenol corresponding to minimal formation yields of 0.04–0.06 and 0.09–0.14, respectively, for the range of reacted phenol in this study. Only in the presence of large NO_2 concentrations, absorptions were visibly assigned to *o*-nitrophenol. Because of the low *p*-benzoquinone and *o*-nitrophenol concentrations, on-line GC-MS measurements using ion traces had to be chosen for quantitative detection. Note, as a result of on-line GC-MS measurements, there was no experimental evidence for the formation of 3-nitrocatechol and *p*-nitrophenol as detected in cryo-trapping experiments. Either both substances were formed below the detection limits or effective wall losses prevented an identification using this technique.

Influence of the NO concentration

In Fig. 4 the obtained product yields for different initial NO concentration are given ($T = 295\text{ K}$, $[\text{O}_2] = 1.68 \times 10^{18}\text{ molecule cm}^{-3}$, $[\text{NO}] = (9.8\text{--}244) \times 10^{12}\text{ molecule cm}^{-3}$). The catechol yield of 0.73 ± 0.04 (2σ limits) was found to be independent of NO concentration. Assuming for the highest NO concentration a contribution of the NO reaction to the conversion of the OH/phenol adduct *via* pathway (5) of less than 10% in competition to the O_2 reaction *via* pathway (3), $k_3/k_5 > 10^{-3}$ at 295 K can be estimated. Using the literature data, $k_3 = (3.0 \pm 0.7) \times 10^{-14}\text{ cm}^3\text{ molecule}^{-1}\text{ s}^{-1}$ (323 K)¹⁰ and $k_5 < 7 \times 10^{-14}\text{ cm}^3\text{ molecule}^{-1}\text{ s}^{-1}$ ($316\text{--}332\text{ K}$)^{9,10} $k_3/k_5 > 0.4$ follows consistent with the ratio obtained in this study. For *o*-nitrophenol and *p*-benzoquinone, because of relatively large scatter no dependency on the NO concentration was detectable, *cf.* Fig. 4. The averaged yields were 0.036 ± 0.017 and 0.012 ± 0.006 , respectively. A NO_2 source under these experimental conditions was the OH generation *via* pathway (10) and the NO_2 levels were at least in the same

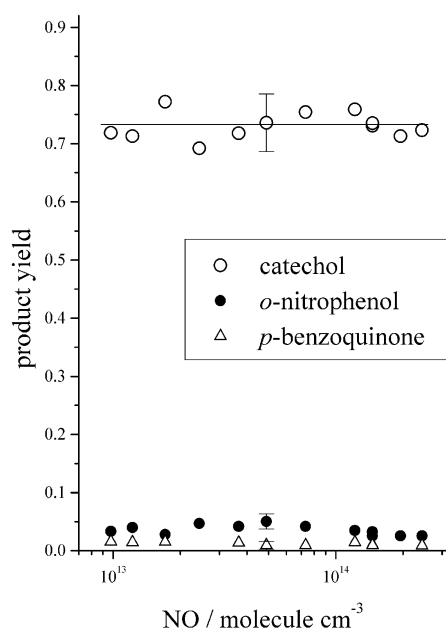


Fig. 4 Product yields in the presence of O_2 determined for different initial NO concentrations; $T = 295\text{ K}$.

dimension as the amount of reacted phenol. Experimentally obtained ratios $[\text{NO}_2]/\Delta[\text{phenol}]$ from FT-IR measurements increased from 1.11 to 1.77 with increasing NO concentration indicating the occurrence of other NO_2 producing steps than pathway (10). The highest NO_2 concentration obtained for the maximum NO addition was $1.2 \times 10^{13}\text{ molecule cm}^{-3}$.

Influence of the NO_2 concentration

In the next set of experiments the influence of the NO_2 concentration on the product yields was investigated ($T = 295\text{ K}$, $[\text{O}_2] = 1.68 \times 10^{18}\text{ molecule cm}^{-3}$, $[\text{NO}] = 1.2 \times 10^{13}\text{ molecule cm}^{-3}$, $[\text{NO}_2] = (7.0\text{--}141) \times 10^{12}\text{ molecule cm}^{-3}$). Even for the highest NO_2 concentration the reaction with H-atoms was of minor importance; lifetime of H-atoms with respect to the reaction with NO_2 *via* pathway (11) $5.5 \times 10^{-5}\text{ s}$ (for the O_2 reaction $4 \times 10^{-6}\text{ s}$). The rate constant $k_{11} = 1.3 \times 10^{-10}\text{ cm}^3\text{ molecule}^{-1}\text{ s}^{-1}$ was taken from the literature.²⁷ Fig. 5 shows the product yields obtained for varying initial NO_2 concentration. Up to NO_2 concentrations of $(3\text{--}4) \times 10^{13}\text{ molecule cm}^{-3}$ the catechol yield was nearly constant. For further increasing NO_2 concentrations, a small but significant decrease of the catechol yield was detectable. The yield of *o*-nitrophenol, however, showed nearly an inverse behaviour. The *p*-benzoquinone yield remained unaffected by NO_2 with an averaged value of 0.010 ± 0.005 .

An attempt was undertaken to estimate the rate constant ratio k_3/k_4 from the measured catechol yields in dependence on NO_2 concentrations for constant O_2 concentration assuming that catechol only came from the OH/phenol adduct. First, it was investigated whether catechol was also formed in the reaction of the OH/phenol adduct with NO_2 or not.

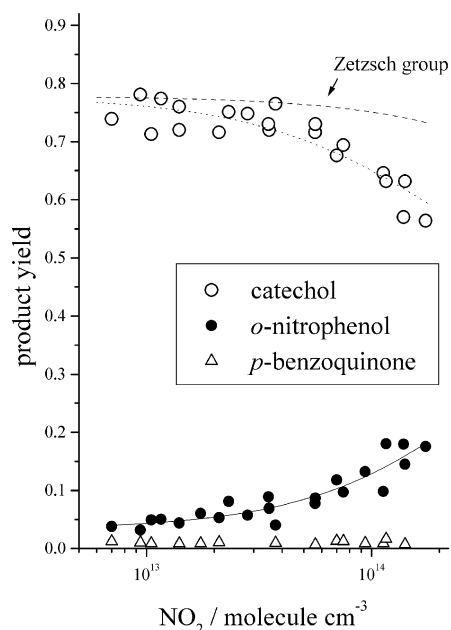
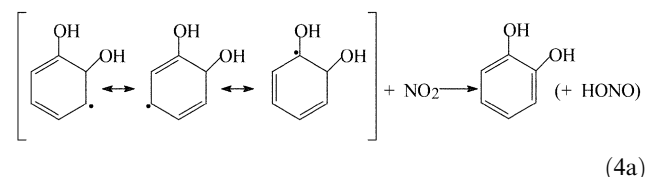


Fig. 5 Product yields in the presence of O_2 obtained by varying the initial NO_2 concentration; $T = 295\text{ K}$, $[\text{NO}] = 1.2 \times 10^{13}\text{ molecule cm}^{-3}$. The dotted line depicts the modeled catechol yield according to eqn. (III), see text. For comparison, the dashed line shows the modeled catechol yield using the rate constants k_3 and k_4 from the Zetzsch group.^{9,10}

Under conditions of a preferred reaction of the OH/phenol adduct with NO₂, a catechol yield of 0.35 ± 0.03 was measured, see later. With the help of pathways (1)–(4) including (3a) and (4a), this yield corresponds to $\frac{k_1}{k_1+k_2} \frac{k_{4a}}{k_4}$ and the total catechol yield can be described in the following way:

$$Y_{\text{catechol}} = \frac{k_1}{k_1+k_2} \left(\frac{k_{3a}}{k_3} / \left(1 + \frac{k_3[\text{O}_2]}{k_4[\text{NO}_2]} \right) + \frac{k_{4a}}{k_4} / \left(1 + \frac{k_4[\text{NO}_2]}{k_3[\text{O}_2]} \right) \right) \quad (\text{III})$$

By means of a procedure for non-linear parameter fitting,¹⁸ setting $\frac{k_1}{k_1+k_2} \frac{k_{4a}}{k_4} = 0.35$, the free parameters $\frac{k_1}{k_1+k_2} \frac{k_{3a}}{k_3}$ and k_3/k_4 from eqn. (III) were estimated to be 0.78 ± 0.02 and $(1.4 \pm 0.5) \times 10^{-4}$, respectively (2σ limits). The first free parameter corresponds to the catechol yield under conditions of a sole catechol formation *via* pathway (3a) and is in good agreement with the obtained catechol yield from experiments with NO additions, *cf.* Fig. 4. In Fig. 5 the dotted line depicts the modeled catechol yield according to eqn. (III). For comparison, the literature data $k_3 = (3.0 \pm 0.7) \times 10^{-14} \text{ cm}^3 \text{ molecule}^{-1} \text{ s}^{-1}$ (323 K)¹⁰ and $k_4 = (3.4 \pm 0.6) \times 10^{-11} \text{ cm}^3 \text{ molecule}^{-1} \text{ s}^{-1}$ (331 K)^{9,10} result in a ratio $k_3/k_4 = (8.8 \pm 2.6) \times 10^{-4}$. This is significantly higher compared to value of this study, $k_3/k_4 = (1.4 \pm 0.5) \times 10^{-4}$. The dashed line (Zetzsch group) in Fig. 5 shows the modeling curve of the catechol yield using k_3/k_4 from the literature^{9,10} and the other parameters as before. A reason for the discrepancy can not be given. Determinations of k_3 and k_4 for different temperatures yielded a small or negligible temperature dependence.^{9,10} So, the higher literature value for k_3/k_4 can not be explained by the higher temperature used in the experiments from the Zetzsch group.

Gas-phase products in the absence of O₂

As a result of the experiments given before, with increasing NO₂ there was a decrease of the catechol yield and at the same time an increase of the *o*-nitrophenol yield, *cf.* Fig. 5. Experiments in the absence of O₂ were conducted to find out the product distribution under conditions of a preferred reaction of the OH/phenol adduct with NO₂ ($T = 295 \text{ K}$, $[\text{NO}_2] = (1.8\text{--}17.2) \times 10^{13} \text{ molecule cm}^{-3}$, Ar as the carrier gas). The initial phenol concentration was $5.9 \times 10^{13} \text{ molecule cm}^{-3}$ and the amount of reacted phenol $(5.9\text{--}8.9) \times 10^{12} \text{ molecule cm}^{-3}$. OH radicals were produced from the reaction of H-atoms with NO₂ *via* pathway (11). Using the rate constants as mentioned above, the H-atom lifetimes with respect to the reaction with NO₂ *via* pathway (11) and with phenol *via* pathway (14) were $\leq 4 \times 10^{-4} \text{ s}$ and 0.07 s , respectively, making the latter step negligible. Fig. 6 shows the product yields for varying initial NO₂ concentration. With increasing NO₂ the catechol yield increased and for $[\text{NO}_2] > 4 \times 10^{13} \text{ molecule cm}^{-3}$ a constant yield of 0.35 ± 0.03 was measured. This behaviour can be tentatively explained by the formation of catechol *via* pathway (4a) to be in competition mainly with the self reaction of the OH/phenol adduct. It is to be noted, that the HONO formation pointed out in pathway (4a) was not experimentally proved. For *o*-nitrophenol, the formation yield increased continuously with increasing NO₂ in the whole NO₂ range. A comparison of the shape of the curves describing the yields for catechol and *o*-nitrophenol shows that both substances were not produced in a simple parallel process starting from the OH/phenol adduct, *cf.* Fig. 6. On the other hand, the NO₂ dependent yields of *o*-nitrophenol in the absence of O₂ (Fig. 6) and in the presence of O₂ (Fig. 5) are in reasonable agreement. From these facts it can be speculated that *o*-nitrophenol was formed from phenoxy radicals *via* pathway (7a). The influence of the NO₂ concentration on the *o*-nitrophenol yield can be described by pathway (7a) to be in competition

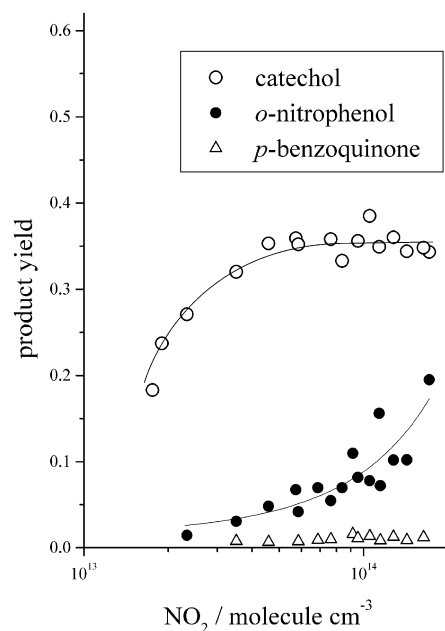


Fig. 6 Product yields in the absence of O₂ obtained by varying the initial NO₂ concentration; $T = 295 \text{ K}$.

with the reaction of phenoxy radicals with other intermediates including the self reaction. The *p*-benzoquinone yield showed an apparent, slight increase with increasing NO₂ concentrations. Because of the insignificance of this effect, only the averaged value of 0.010 ± 0.006 can be given.

Temperature dependence of the product yields

In the temperature range of 266–364 K, product yields were measured for constant initial mole fractions of the reactants (concentrations calculated for $T = 295 \text{ K}$, $[\text{O}_2] = 1.68 \times 10^{18} \text{ molecule cm}^{-3}$, $[\text{NO}] = 4.9 \times 10^{13} \text{ molecule cm}^{-3}$, $[\text{phenol}] = (6.6\text{--}6.7) \times 10^{13} \text{ molecule cm}^{-3}$). The amount of reacted phenol was in the range $(5.4\text{--}7.2) \times 10^{12} \text{ molecule cm}^{-3}$. Because k_3 and k_4 are weakly temperature-dependent,^{9,10} in the whole temperature range the fate of the OH/phenol adduct was governed by the reaction with O₂ *via* pathway (3). Fig. 7 depicts the experimental findings. The catechol yield showed a distinct increase with increasing temperature, 0.37 ± 0.06 for 266 K and 0.87 ± 0.04 for 364 K. In principle, a similar behaviour was found for the phenol yield from the reaction of OH radicals with benzene.⁶ Because in eqn. (I) $k_{13,\text{catechol}}/k_{12}$ was assumed to be temperature-independent, the determination of the catechol yield *via* eqn. (I) was probably incorrect. In Fig. 7 the averaged “raw data” of the catechol yield determined by neglecting pathway (13), $Y_{\text{catechol}} = [\text{catechol}]/\Delta[\text{phenol}]$, are also given as lower limit. From kinetic data,¹⁰ the formation yield of the OH/phenol adduct, $k_1/(k_1+k_2)$, can be expected to be 0.7 at 364 K and by extrapolation 0.8 at 266 K. Other kinetic data from the same group⁹ yield somewhat different estimates for the OH/phenol adduct yields (0.74 at 364 K and 0.91 at 266 K). From the observed catechol yields above 320 K of approximately 0.85 (raw data: 0.72), *cf.* Fig. 7, it can be speculated that under these conditions the OH/phenol adduct is mainly converted to catechol *via* pathway (3a). Starting from 320 K, with decreasing temperature other steps than pathway (3a) become more important for the fate of the OH/phenol adduct. In contrast to catechol, for the yields of *o*-nitrophenol and *p*-benzoquinone there was no temperature effect detectable. The averaged yields were 0.043 ± 0.017 and 0.012 ± 0.006 , respectively. Summarising the formation yields, the gas-phase products accounted for $92 \pm 6\%$ of

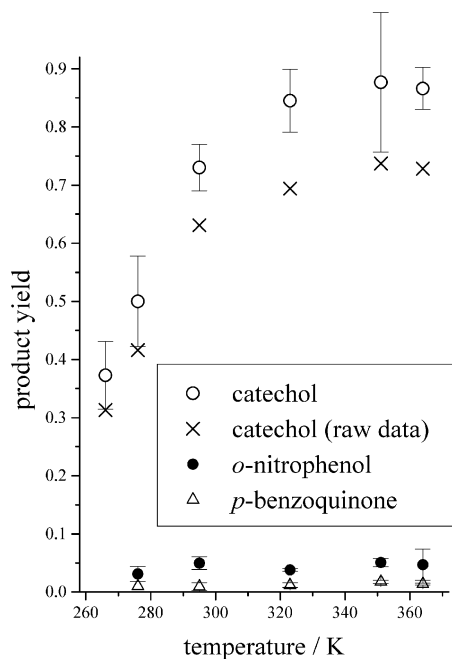


Fig. 7 Temperature-dependent product yields in the presence of O_2 measured for constant initial mole fractions; $[NO] = 4.9 \times 10^{13}$ molecule cm^{-3} (calculated for 295 K). The “raw data” of the catechol yield stand for values not corrected for the consecutive reaction with OH, see text.

the carbon of the reacted phenol at 364 K and $42 \pm 8\%$ at 266 K.

Particle formation

As discussed in the paragraph before, with decreasing temperature there was an increasing lack of carbon in the observed gas-phase products. A possible explanation for this behaviour is the enhanced occurrence of condensable products at lower temperature and the formation of particles. Particle measurements were performed in the temperature range of 275–295 K using again constant initial mole fractions of the reactants (concentrations calculated for $T = 295$ K, $[O_2] = 1.68 \times 10^{18}$ molecule cm^{-3} , $[NO] = 1.2 \times 10^{13}$ molecule cm^{-3} , $[phenol] = 6.4 \times 10^{13}$ molecule cm^{-3}). In Fig. 8 the measured particle numbers for four different amounts of converted phenol for different temperatures are plotted. The varying amounts of converted phenol were achieved changing the H_2 contents in the gas stream for the microwave discharge and so the amount of OH radicals. The observed number of newly formed particles in this system was found to be strongly dependent on temperature and the amount of reacted phenol. The temperature effect can be explained that with decreasing temperature probably more condensable species are formed and/or the saturation vapour pressure of the condensable species is going down supporting the nucleation process. The observed number of formed particles for different gas-phase concentration of the condensable species for constant time can be explained tentatively by eqn. (IV).²⁸

$$N = P c_{\text{condens}}^n \quad (\text{IV})$$

N stands for the number of formed particles, c_{condens} for the gas-phase concentration of the condensable species, n and P are free parameters. Under conditions of a kinetically controlled nucleation process, n characterises the number of molecules in the critical cluster. Assuming that c_{condens} represents a constant fraction of the reacted phenol for a fixed temperature, from measurements at 283 K ($N = 500$, 1.1×10^4 and 5×10^4 (estimate) cm^{-3} for $\Delta[phenol] = 4.8 \times 10^{12}$, 5.8×10^{12} and

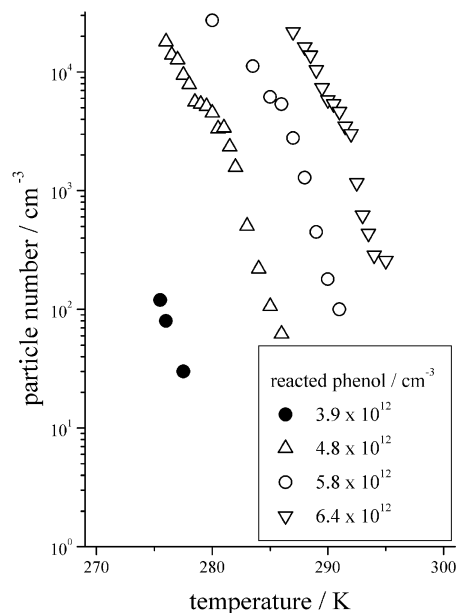


Fig. 8 Measured particle numbers ($d > 15$ nm) for constant initial mole fractions in dependence on temperature and the amount of reacted phenol; $[NO] = 1.2 \times 10^{13}$ molecule cm^{-3} , $[O_2] = 1.68 \times 10^{18}$ molecule cm^{-3} (calculated for 295 K).

6.4×10^{12} molecule cm^{-3} , respectively) $n = 16$ was found. A power of 16 in this nucleation law demonstrates the extremely strong increase of the number of formed particles with increasing concentration of the condensable species. Because n was determined just for a single temperature, the found value can be regarded only as a rough estimate. For the nucleation of sulfuric acid, $n = 7$ –13 in dependence on the humidity in the system was experimentally observed.²⁸ For the chemical nature of the nucleating substances in the phenol system, there exists no reasoning. To the best of our knowledge, there is no information available in the literature describing the formation of condensable substances from the reaction of OH radicals with phenol.

The particle measurements showed that with decreasing temperature the particle number increased. That helps to fulfil the carbon balance, at least qualitatively.

Summary and application to the atmosphere

In Table 1 experimentally obtained product yields from the gas-phase reaction of OH radicals with phenol from the literature along with the results of this study are given. For NO_2 concentrations $< (3\text{--}4) \times 10^{13}$ molecule cm^{-3} and room temperature, the catechol yield of 0.73–0.78 was found to be in good agreement with the result of a chamber study, (0.804 ± 0.121) .¹³ The formation of catechol can be described by the reaction of O_2 with the OH/phenol adduct *via* pathway (3a). Because under realistic atmospheric conditions the fate of the OH/phenol adduct is also governed by pathway (3a) and no pressure effects can be expected, the catechol yield of 0.73–0.78 (295 K) is applicable for atmospheric conditions. Considering the formation of phenol from the reaction of OH radicals with benzene with a yield of 0.24–0.53^{3–6} at room temperature, the main products of the OH radical initiated degradation of these simple aromatics in the atmosphere are the corresponding hydroxylated species each.

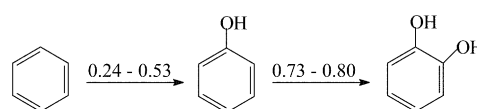


Table 1 Compilation of product yields

Pressure/mbar	Temperature/K	Initial concentrations/ molecule cm ⁻³	Product yields			Source
			Catechol	<i>o</i> -Nitrophenol	<i>p</i> -Benzoquinone	
~990 synthetic air	296 ± 2	Phenol: (1.5–2.8) × 10 ¹³ NO: 2.4 × 10 ¹⁴	—	0.067 ± 0.015	—	Ref. 7
1000 synthetic air	298 ± 2	Phenol: (2.6–10.8) × 10 ¹³ NO: (1.2–4.2) × 10 ¹³	0.804 ± 0.121	0.058 ± 0.010	0.037 ± 0.012	Ref. 13
100	295	Phenol: 6.5 × 10 ¹³ O ₂ : 1.68 × 10 ¹⁸ NO: (9.8–244) × 10 ¹²	0.73 ± 0.04	0.036 ± 0.017	0.012 ± 0.006	This study
100	295	Phenol: 6.5 × 10 ¹³ O ₂ : 1.68 × 10 ¹⁸ NO: 1.2 × 10 ¹³ NO ₂ : (7.0–141) × 10 ¹²	NO ₂ -dependent (0.78 ± 0.02 for [NO ₂] → 0)	NO ₂ -dependent	0.010 ± 0.005	This study
100	295	Phenol: 5.9 × 10 ¹³ O ₂ : <2 × 10 ¹³ NO ₂ : (1.8–17.2) × 10 ¹³	NO ₂ -dependent (0.35 ± 0.03 for [NO ₂] > 4 × 10 ¹³)	NO ₂ -dependent	0.010 ± 0.006	This study
100	266–364	^a Phenol: (6.6–6.7) × 10 ¹³ ^a O ₂ : 1.68 × 10 ¹⁸ ^a NO: 4.9 × 10 ¹³	<i>T</i> -dependent	0.043 ± 0.017	0.012 ± 0.006	This study

^a Calculated for 295 K.

The temperature-dependent measurements showed a clear decrease of the catechol yield with decreasing temperature.

The observed formation of *o*-nitrophenol was found to be dependent on the NO₂ concentration but independent on O₂, cf. Fig. 5 and 6. At least for relatively low NO₂ concentrations, [NO₂] < 2 × 10¹³ molecule cm⁻³, it seems to be likely that *o*-nitrophenol was formed from the reaction of NO₂ with phenoxy radicals *via* pathway (7a). It is not clear whether the observed *o*-nitrophenol yields (0.067 ± 0.015 from ref. 7, 0.058 ± 0.010 from ref. 13 and 0.036 ± 0.017 from this study) can be applied for realistic atmospheric conditions with NO₂ concentrations of approximately 5 × 10¹¹ molecule cm⁻³ (atmospheric mixing ratio: 20 ppb). In the real atmosphere, phenoxy radicals react probably also with O₃ or other species in competition to the reaction with NO_x.¹² To clarify that, more experimental work is needed concerning the atmospheric fate of phenoxy radicals.

The detected yield of *p*-benzoquinone was not influenced by experimental conditions (NO, NO₂, O₂, temperature) and there were no indications for the formation pathways of this substance. Therefore, as a result of this study, a discussion of the atmospheric relevance of the *p*-benzoquinone yield is highly speculative.

The measured dependence of the catechol yield on NO and NO₂ for constant O₂ concentrations allowed an estimate of the reactivity of the OH/phenol adduct towards O₂, NO and NO₂, $k_3/k_5 > 10^{-3}$ and $k_3/k_4 = (1.4 \pm 0.5) \times 10^{-4}$. As compared with literature data,^{9,10} the latter ratio is smaller by a factor of six. Nevertheless, this estimate confirms the fact that under atmospheric conditions the OH/phenol adduct reacts exclusively with O₂.

For evaluation of a possible competing process under the experimental conditions used, the rate constant for H + phenol was measured, $k_{14} = (2.5 \pm 1.5) \times 10^{-13}$ cm³ molecule⁻¹ s⁻¹ (295 ± 2 K, 25 mbar He), representing the first determination of this value at room temperature.

Acknowledgements

The authors thank Markus Hermann and Jost Heintzenberg for help during the particle measurements, Frank Stratmann and Cornelius Zetzsch for useful discussions, and Herwig Macholeth for technical assistance.

References

- B. J. Finlayson-Pitts and J. N. Pitts, Jr., in *Chemistry of the Upper and Lower Atmosphere*, Academic Press, 2000.
- R. Atkinson, *J. Phys. Chem. Ref. Data*, 1994, Monograph No. 2, 47.
- R. Atkinson, S. M. Aschmann, J. Arey and W. P. L. Carter, *Int. J. Chem. Kinet.*, 1989, **21**, 801; reassessment in: R. Atkinson and S. M. Aschmann, *Int. J. Chem. Kinet.*, 1994, **26**, 929.
- B. Bohn, M. Elend and C. Zetzsch, in *CMD Annual Report 98*, ed. EUROTRAC-2 International Scientific Secretariat, Munich, 1999, p. 112.
- R. Volkamer, B. Klotz, I. Barnes, T. Imamura, K. Wirtz, N. Washida, K. H. Becker and U. Platt, *Phys. Chem. Chem. Phys.*, 2002, **4**, 1598.
- T. Berndt and O. Böge, *Phys. Chem. Chem. Phys.*, 2001, **3**, 4946.
- R. Atkinson, S. M. Aschmann and J. Arey, *Environ. Sci. Technol.*, 1992, **26**, 1397.
- R. Atkinson, *J. Phys. Chem. Ref. Data*, 1989, Monograph No. 1, 231.
- R. Knispel, R. Koch, M. Siese and C. Zetzsch, *Ber. Bunsen-Ges. Phys. Chem.*, 1990, **94**, 1375.
- R. Koch, *Ph.D. Thesis*, Hannover, 1992; R. Koch, J. Nowack, M. Siese and C. Zetzsch, in *Proc. CEC/EUROTRAC Discussion Meeting*, York, 1991.
- F. Berho and R. Lesclaux, *Chem. Phys. Lett.*, 1997, **279**, 289.
- J. Platz, O. J. Nielsen, T. J. Wallington, J. C. Ball, M. D. Hurley, A. M. Straccia, W. F. Schneider and J. Sehested, *J. Phys. Chem. A*, 1998, **102**, 7964.
- R. Olariu, B. Klotz, I. Barnes, K. H. Becker and R. Mocanu, *Atmos. Environ.*, 2002, **36**, 3685.
- P. Barzaghi and H. Herrmann, *Phys. Chem. Chem. Phys.*, 2002, **4**, 3669.
- C. A. Brock, J. C. Wilson, D. W. Gesler, B. G. Lafleur and J. M. Reeves, in *AGU Fall Meet. Suppl. (abstracts)*, San Francisco, 1998, p. F138.
- M. Hermann and J. Heintzenberg, private communication.
- M. Hermann and A. Wiedensohler, *J. Aerosol. Sci.*, 2001, **32**, 975.
- J. Stoer and R. Bulirsch, *Einführung in die Numerische Mathematik II*, Springer Verlag, Berlin, 1978.
- M. Rinke and C. Zetzsch, *Ber. Bunsen-Ges. Phys. Chem.*, 1984, **88**, 55.
- R. I. Olariu, I. Barnes, K. H. Becker and B. Klotz, *Int. J. Chem. Kinet.*, 2000, **32**, 696.
- M. Semadeni, D. W. Stocker and J. A. Kerr, *Int. J. Chem. Kinet.*, 1995, **27**, 287.
- T. Berndt and O. Böge, *Int. J. Chem. Kinet.*, 2001, **33**, 124.
- G. Berti, *Gazz. Chim. Ital.*, 1957, **87**, 659.

- 24 D. L. Baulch, C. J. Cobos, R. A. Cox, C. Esser, P. Frank, Th. Just, J. A. Kerr, M. J. Pilling, J. Troe, R. W. Walker and J. Warnatz, *J. Phys. Chem. Ref. Data*, 1992, **21**, 411.
- 25 J. M. Nicovich and A. R. Ravishankara, *J. Phys. Chem.*, 1984, **88**, 2534.
- 26 K. J. Hsu, J. L. Durant and F. Kaufman, *J. Phys. Chem.*, 1987, **91**, 1895.
- 27 H. Gg. Wagner, U. Welzbach and R. Zellner, *Ber. Bunsen-Ges. Phys. Chem.*, 1976, **80**, 1023.
- 28 S. M. Ball, D. R. Hanson, F. L. Eisele and P. H. McMurry, *J. Geophys. Res.*, 1999, **104**, 23 709.